Eur. Phys. J. A **20**, 69–73 (2004)
DOI 10.1140/epja/i2003-10201-5

THE EUROPEAN PHYSICAL JOURNAL A

Shell model results for exotic nuclei

T. Otsuka[a]

Department of Physics, University of Tokyo, Hongo, Tokyo 113-0033, Japan and RIKEN, Hirosawa, Wako-shi, Saitama 351-0198, Japan and Center for Nuclear Study, University of Tokyo, Hongo, Tokyo 113-0033, Japan

Received: 10 January 2003 /
Published online: 9 March 2004 –

Abstract. Recent developments of the nuclear shell model are presented. The magic numbers are the key concept of the shell model, and are shown to be different in exotic nuclei from those of stable nuclei. Their novel origin and robustness will be discussed. By the Monte Carlo Shell Model (MCSM), the structure of low-lying states can be studied with realistic interactions for a wide variety of nuclei. Some examples are discussed in connection to the triaxial deformation and a narrow shell gap at $N = 20$ for Z smaller.

PACS. 21.60.Cs Shell model – 21.30.Fe Forces in hadronic systems and effective interactions – 13.75.Cs Nucleon-nucleon interactions (including antinucleons, deuterons, etc.) – 21.10.-k Properties of nuclei; nuclear energy levels

1 Introduction

I shall discuss, in this paper, our recent results on shell model studies of exotic nuclei, indicating that the shell, or magic, structure can be varied in going from stable to exotic nuclei and such a change is strongly related to certain properties of the nucleon-nucleon interaction [1]. I shall propose a paradigm of shell evolution as one of the key principles in determining the structure of exotic nuclei [2].

The magic numbers play a key role in many-body physics as the most fundamental quantity reflecting possible shell structure. The nuclear shell model has been started by Mayer and Jensen by identifying its magic numbers and their origin [3]. The study of nuclear structure has advanced on the basis of the shell structure thus clarified. Shell-model studies, on the other hand, have been made predominantly for stable nuclei, which are on or near the β-stability line in the nuclear chart. This is basically because only those nuclei have been accessible experimentally. In such stable nuclei, the magic numbers suggested by Mayer and Jensen remain valid, and the shell structure can be understood well in terms of the harmonic-oscillator potential with a spin-orbit splitting.

Recently, studies on exotic nuclei far from the β-stability line have started owing to the development of radioactive nuclear beams, as discussed also in this conference. The magic numbers in such exotic nuclei can be a quite intriguing issue. I shall show that new magic numbers appear and some other conventional ones disappear in moving from stable to exotic nuclei in a rather novel manner due to a particular part of the nucleon-nucleon interaction [1,2]. Although the magic numbers are prominent features, there are gradual changes of underlying single-particle or shell structure. Including those changes, I would like to call these phenomena "Shell Evolution".

If single-particle energies are calculated by the Woods-Saxon potential, they change as the proton number (Z) or the neutron number (N) varies. In this case, the single-particle energies are shifted basically in parallel, keeping their relative energies (or mutual differences of the energies) almost unchanged. This kind of change is due to the variation of the potential radius depending on A ($= N+Z$) and/or the shift of the potential depth associated with N/Z asymmetry, and is not called Shell Evolution. Note that, even with the Woods-Saxon potential, the relative energies can be changed near drip lines owing to varying influences of the centrifugal potential, but such changes are not the subject of this paper, and may be better referred to with a different nomenclature because of their kinetic origin.

Shell Evolution means that the relative energies can vary rather significantly as N and/or Z change. If this energy change becomes sufficiently significant, even the shell gap can disappear or a new gap may arise. Thus, as a result of the Shell Evolution, the magic numbers may change.

The Shell Evolution has been seen in the p-shell and sd-shell already [1]. In order to understand it, we use effective single-particle energies as explained in sect. 2. The Shell Evolution seems to occur, in many cases, due to the common mechanism related to the Nucleon-Nucleon (NN) interaction as discussed in sects. 3 and 4. Because of this generality and robustness, one can raise the paradigm

[a] e-mail: otsuka@phys.s.u-tokyo.ac.jp

of the Shell Evolution as an underlying principle determining the structure of exotic nuclei.

2 Effective single-particle energies

In order to understand the underlying single-particle properties of a nucleus, we can make use of *effective (spherical) single-particle energies (ESPEs)*, which represent mean effects from the other nucleons on a nucleon in a specified single-particle orbit.

In the shell model, single-particle orbits are classified into two groups. One is for the orbits in the inert core, which is a closed shell. The other is for the orbits outside the inert core, and valence nucleons are moving on those orbits. Here, we are discussing spherical single-particle orbits with good orbital and total angular momenta, l and j. Each orbit has its single-particle energy. This energy contains the kinetic energy and the binding from the nucleons in the inert core. For nuclei consisting of the inert core and only one more nucleon (like ^{17}O), these single-particle energies give the energy levels of the nucleus unless the inert core is broken. In the usual shell model calculations, these single-particle energies are called *bare* single-particle energies.

As one adds more valence nucleons on top of the inert core, effects of the so-called residual interaction become larger. The shell-model (residual) interaction between valence nucleons includes various multipole components. We shall discuss on them. The quadrupole component, for instance, is the origin of the quadrupole collectivity producing vibrational and rotational spectra. To be intuitive, the quadrupole component produces more binding energy, when the relative angle (with respect to the center of the nucleus) between two interacting nucleons is smaller, *i.e.*, two nucleons are correlated in angle. By making such a correlation collective, one comes to a deformed shape. For instance, in the case of a prolate shape, valence nucleons are gathered near the longer axis.

In contrast, in the monopole component, effects depending on this relative angle between valence nucleons are averaged out. Namely, the monopole component does not care how far the two interacting nucleons are in angle.

We next discuss how to calculate the monopole component. The two-body matrix element of the interaction depends on the angular momentum J, coupled by the two interacting nucleons in orbits j_1 and j_2. This J-dependence is averaged out with a weight factor $(2J+1)$. Since mean effects are being considered, only diagonal matrix elements are taken. The monopole interaction is thus obtained with a matrix element [4,5]:

$$V^T_{j_1 j_2} = \frac{\sum_J (2J+1)\langle j_1 j_2|V|j_1 j_2\rangle_{JT}}{\sum_J (2J+1)}, \quad \text{for } T=0,\ 1, \quad (1)$$

where $\langle j_1 j_2|V|j_1' j_2'\rangle_{JT}$ stands for the matrix element of a two-body interaction, V. Although this is still a two-body interaction, it has no dependence on J. Here, the isospin dependence, $T = 0$ or 1, is kept, however.

We point out an important property of the monopole interaction. Since the angular correlation is taken away, two nucleons can be at any magnetic substate, yielding the same binding energy. So, in evaluating its effects in a system with many valence nucleons, only the number of nucleons in each orbit matters. This implies that the effect of the monopole interaction can be accumulated, and therefore, its effect becomes the largest when the orbit is fully occupied. On the other hand, this is not the case for other multipoles, and the effects vanish for fully occupied orbits. Mathematically, the monopole operator has a finite trace, whereas the trace is zero for other multipoles. Thus, even a weak monopole interaction can be magnified in its effect by a large number of nucleons.

The monopole Hamiltonian consists of the bare single-particle energies stated above and the monopole interaction (between valence nucleons).

The ESPE is evaluated from this monopole Hamiltonian, and can naturally play the role of a measure of mean effects from the other nucleons, including the valence ones. For simplicity, the normal filling configuration is used. Note once again that, because the J-dependence is taken away, only the number of nucleons in each orbit matters. As a natural assumption, the lowest possible isospin coupling is considered for protons and neutrons in the same orbit. The ESPE of an *occupied* orbit is defined to be the separation energy of this orbit with the opposite sign. Note that the separation energy implies the minimum energy needed to take a nucleon out of this orbit. The ESPE of an *unoccupied* orbit is defined to be the binding energy gain by putting a proton or neutron into this orbit with the opposite sign.

Thus, effective single-particle energies can be defined and we now use them. In actual calculations, the isospin coupling must be considered between the two orbits in the monopole Hamiltonian, but this is a rather theoretical detail and is not discussed here (see eq. (1) of [5], for example).

3 The shell gap at N = 16

We now show ESPEs for a stable nucleus (^{30}Si) and for an exotic nucleus (^{24}O) in fig. 1(a) and (b), respectively. The shell model Hamiltonian is the one derived in [5]. This Hamiltonian produces quite good agreement with experiment for a large number of nuclei within a single framework [5,6].

In fig. 1(b), shown are ESPEs for ^{24}O, where the $0d_{3/2}$ is lying much higher, very close to the pf shell. A considerable gap ($\sim$ 4 MeV) is observed between the $0d_{3/2}$ and the pf shell for the stable nucleus ^{30}Si, whereas an even larger gap ($\sim$ 6 MeV) is found between $0d_{3/2}$ and $1s_{1/2}$ for ^{24}O. The basic mechanism of this dramatic change is the strongly attractive interaction shown schematically in fig. 1(c), where $j_> = l+1/2$ and $j_< = l-1/2$ with l being the orbital angular momentum. In the present case, $l = 2$. One now should remember that valence protons are added into the $0d_{5/2}$ orbit as Z increases from 8 to 14. Due to a

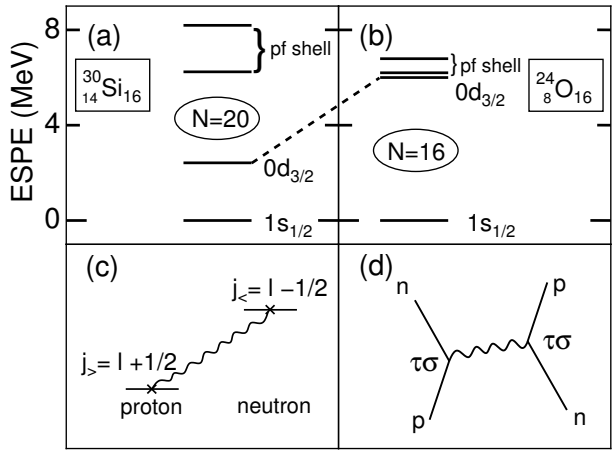

Fig. 1. ESPEs for (a) ^{30}Si and (b) ^{24}O, relative to $0d_{5/2}$. The dashed line connecting (a) and (b) is drawn to indicate the change of the $0d_{3/2}$ level. (c) The major interaction producing the change between (a) and (b). (d) The elementary process relevant to the interaction in (c). Taken from [1].

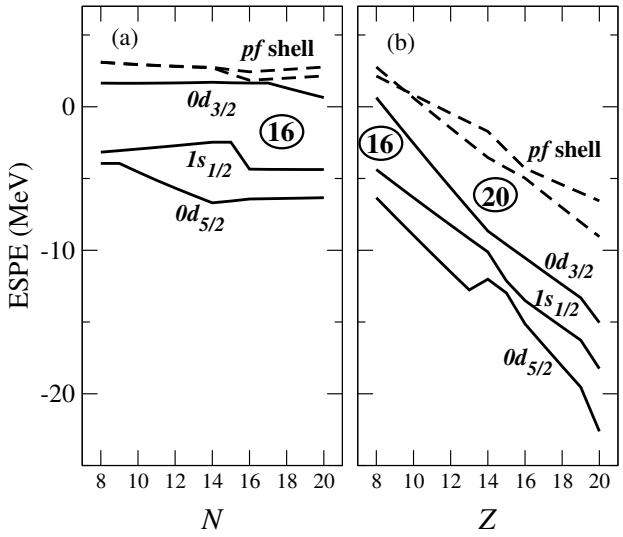

Fig. 2. Effective single-particle energies of neutrons for (a) oxygen isotopes from $N = 8$ to 20 and (b) $N = 20$ isotones from $Z = 8$ to 20. Taken from [7].

strong attraction between a proton in $0d_{5/2}$ and a neutron in $0d_{3/2}$, as more protons are put into $0d_{5/2}$, a neutron in $0d_{3/2}$ is more strongly bound. Thus, the $0d_{3/2}$ ESPE for neutrons is so low in ^{30}Si as compared to that in ^{24}O.

4 Spin-isospin dependence in the NN interaction

The process illustrated in fig. 1(d) produces the attractive interaction in fig. 1(c). The NN interaction in this process is written as

$$V_{\tau\sigma} = \tau \cdot \tau \ \sigma \cdot \sigma \ f_{\tau\sigma}(r). \qquad (2)$$

Here, the symbol "$\cdot$" denotes a scalar product, τ and σ stand for isospin and spin operators, respectively, r implies the distance between two interacting nucleons, and $f_{\tau\sigma}$ is a function of r. In the long-range (or no r-dependence) limit of $f_{\tau\sigma}(r)$, the interaction in eq. (2) can couple only a pair of orbits with the same orbital angular momentum l, which are nothing but $j_>$ and $j_<$.

The σ operator couples $j_>$ to $j_<$ (and vice versa) much more strongly than $j_>$ to $j_>$ or $j_<$ to $j_<$. Therefore, the spin-flip process is more favored in the vertices in fig. 1(d). The same mathematical mechanism works for isospin: the τ operator favors charge-exchange processes. Combining these two properties, $V_{\tau\sigma}$ produces large matrix elements for the spin-flip isospin-flip processes: proton in $j_> \rightarrow$ neutron in $j_<$ and vice versa. This gives rise to the interaction in fig. 1(c). This feature is a general one and is maintained with $f_{\tau\sigma}(r)$ in eq. (2) with reasonable r-dependences.

Although $V_{\tau\sigma}$ yields sizable attraction between a proton in $j_>$ and a neutron also in $j_>$, the effect is weaker than in the case of fig. 1(c).

In stable nuclei with $N \sim Z$ with ample occupancy of the $j_>$ orbit in the valence shell, the proton (neutron) $j_<$ orbit is lowered by neutrons (protons) in the $j_>$ orbit. In exotic nuclei, this lowering can be absent, and then the $j_<$ orbit is located rather high, not far from the upper shell. In this sense, the proton-neutron $j_>$-$j_<$ interaction enlarges a gap between major shells for stable nuclei with proper occupancy of relevant orbits.

The origin of the strongly attractive $V_{\tau\sigma}$ is quite clear. The One-Boson-Exchange-Potentials (OBEP) for π and ρ mesons have this type of terms as major contributions. While the OBEP is one of the major parts of the effective NN interaction, the effective NN interaction in nuclei can be provided by a G-matrix calculation with core polarization corrections. Such effective NN interaction will be called simply G-matrix interaction for brevity. The G-matrix interaction should maintain the basic features of meson exchange processes, and, in fact, existing G-matrix interactions generally have quite large matrix elements for the cases shown in fig. 1(c) [8].

5 The gap at N = 20 and the structure of N = 20 exotic nuclei

We now turn to exotic nuclei with $N \sim 20$. Figures 2(a) and (b) show the ESPEs of neutrons for oxygen isotopes and $N = 20$ isotones, respectively [7]. The small effective gap between $0d_{3/2}$ and the pf shell for neutrons is seen in oxygen isotopes in fig. 2(a), while this gap becomes wider as Z increases in the $N = 20$ isotones in fig. 2(b). This small gap for smaller Z is nothing but what we have seen for ^{24}O in fig. 1(b). Thus, the disappearance of $N = 20$ magic structure in exotic nuclei with Z much smaller than 20 and the appearance of the new magic structure in ^{24}O [9] have the same origin. Furthermore, one sees a less pronounced gap between $0d_{5/2}$ and $1s_{1/2}$ at $N = 14$ in fig. 2(a). This gap makes ^{22}O a magic-like nucleus [10].

The excitation of neutrons across the $N = 20$ gap produces various deformations. As an example, fig. 3 shows

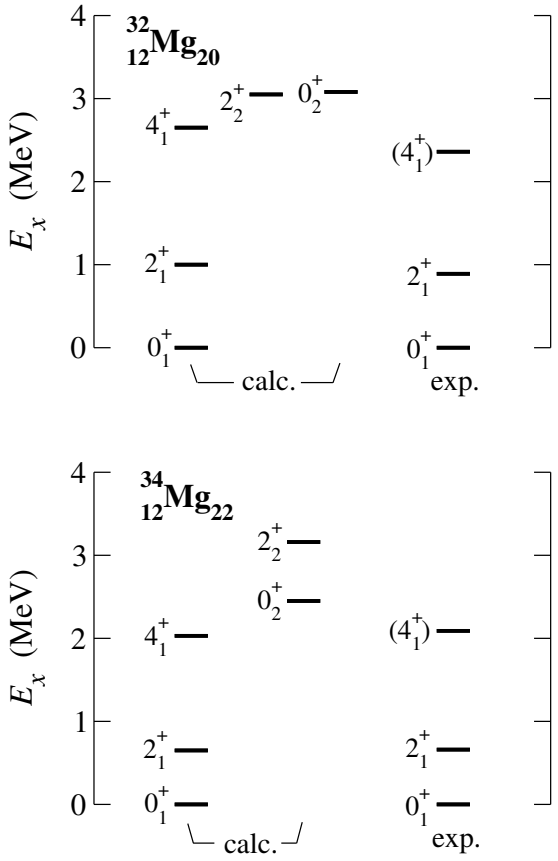

Fig. 3. Level structure of ^{32,34}Mg. Taken from [2].

low-lying energy levels of ^{32,34}Mg. Some levels are known experimentally [11–13], and the agreement is quite good to calculated results obtained by the Monte Carlo Shell Model [5,7,14–16].

The spacing between the 2^+_1 and 4^+_1 can suggest, to a good extent, the shapes of these nuclei, although the 4^+_1 level may be only tentatively known experimentally [11–13]. The ratio between the excitation energies of these two states is 2.65 in ^{32}Mg, suggesting that this nucleus is triaxially deformed [17]. On the other hand, the same ratio becomes 3.1 in ^{34}Mg, suggesting that this nucleus is an axially-symmetric rotor. Such a difference seems to be attributed to the number of neutrons in the pf shell: about two in ^{32}Mg and about four in ^{34}Mg. The latter case can produce the strong prolate deformation within the $f_{7/2}$ orbit, while the former case is not enough to stabilize it and favors an oblate deformation. Therefore, by combining with the prolate deformed proton system in the *sd* shell, ^{34}Mg becomes a prolate axially symmetric rotor, whereas ^{32}Mg tends to be triaxially deformed. I emphasize that the present calculated results are predictions as shown in an earlier reference [5].

The present calculation [5] predicts the $B(E2; 2^+_1 \rightarrow 0^+_1)$ values also quite well in agreement with experimental values [18,19]. Although the $B(E2)$ value has been measured only between the 0^+_1 and 2^+_1 states, the calculated $B(E2; 4^+_1 \rightarrow 2^+_1)$ values suggest the triaxial deformation for ^{32}Mg and the axially symmetric deformation for ^{34}Mg, in a consistent manner with their excitation energies.

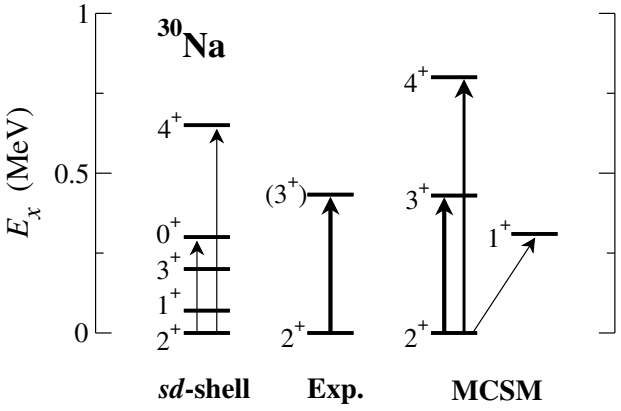

Fig. 4. Level structure of ^{30}Na. Arrows indicate $E2$ transitions with widths proportional to their $B(E2)$ values. Experimental data are taken from [20].

Another example is the level scheme of ^{30}Na shown in fig. 4. One finds a remarkable agreement between the MCSM calculation with the present Hamiltonian and the experiment [20]. On the other hand, in the *sd*-shell model, where only the *sd* shell is taken as the valence shell, only poor agreement can be achieved.

6 Heavier nuclei: N = 34

Moving back to heavier nuclei, from the strong interaction in fig. 1(c), we can predict other magic numbers, for instance, $N = 34$ associated with the $0f_{7/2}$-$0f_{5/2}$ interaction. A recent experiment seems to support $N = 34$ new magic number [21].

7 Summary and perspectives

In summary, we showed how shell structure and magic numbers are changed in nuclei far from the β-stability line: $N = 6$, 16, 34, etc. can become magic numbers in neutron-rich exotic nuclei, while usual magic numbers, $N = 8$, 20, 40, etc., may disappear. The mechanism of this change can be explained by the strong attractive $V_{\tau\sigma}$ interaction which has robust origins in OBEP, G-matrix and QCD. In fact, simple structure features such as magic numbers should have a simple and robust basis. Including other possible origins, I would like to propose that the structure of stable and exotic nuclei should be studied with the paradigm of Shell Evolution where the shell structure (and magic numbers) can vary significantly as results of variable contributions of nucleon-nucleon interaction and many-body dynamics, depending on Z and N.

This work has been a part of the CNS-RIKEN joint research project on nuclear shell model. This work was supported in part by a Grant-in-Aid for Specially Promoted Research (13002001) from the Ministry of Education, Culture, Sports, Science and Technology.

References

1. T. Otsuka, R. Fujimoto, Y. Utsuno, B.A. Brown, M. Honma, T. Mizusaki, Phys. Rev. Lett. **87**, 082502 (2001).
2. T. Otsuka, Prog. Theor. Phys. Suppl. **146**, 6 (2002).
3. M.G. Mayer, Phys. Rev. **75**, 1969 (1949); O. Haxel, J.H.D. Jensen, H.E. Suess, Phys. Rev. **75**, 1766 (1949).
4. A. Poves, A. Zuker, Phys. Rep. **70**, 235 (1981).
5. Y. Utsuno, T. Otsuka, T. Mizusaki, M. Honma, Phys. Rev. C **60**, 054315 (1999).
6. Y. Utsuno, T. Otsuka, T. Mizusaki, M. Honma, Phys. Rev. C **64**, 011301 (2001).
7. T. Otsuka, M. Honma, T. Mizusaki, N. Shimizu, Y. Utsuno, Prog. Part. Nucl. Phys. **47**, 319 (2001).
8. M. Hjorth-Jensen, T.T.S. Kuo, E. Osnes, Phys. Rep. **261**, 125 (1995); M. Hjorth-Jensen, private communication.
9. A. Ozawa *et al.*, Phys. Rev. Lett. **84**, 5493 (2000).
10. P.G. Thirolf *et al.*, Phys. Lett. B **485**, 16 (2000).
11. D. Guillemaud-Mueller *et al.*, Nucl. Phys. A **426**, 37 (1984).
12. A. Azaiez *et al.*, in *Proceedings of the International Conference on Nuclear Structure 98*, edited by C. Baktash, AIP Conf. Proc. **481**, 243 (1999).
13. K. Yoneda *et al.*, Phys. Lett. B **499**, 233 (2001).
14. M. Honma, T. Mizusaki, T. Otsuka, Phys. Rev. Lett. **75**, 1284 (1995).
15. T. Otsuka, M. Honma, T. Mizusaki, Phys. Rev. Lett. **81**, 1588 (1998) and references therein.
16. Y. Utsuno *et al.*, to be published.
17. T. Otsuka, Nucl. Phys. A **616**, 406c (1997).
18. T. Motobayashi *et al.*, Phys. Lett. B **346**, 9 (1995).
19. H. Iwasaki *et al.*, Phys. Lett. B **522**, 227 (2001).
20. B.V. Pritychenko *et al.*, Phys. Rev. C **66**, 024325 (2002).
21. R.V. Janssens *et al.*, Phys. Lett. B **546**, 55 (2002).